Title

The Dual Action of Human Antibodies Specific to *Plasmodium falciparum* PfRH5 and PfCyRPA: Blocking Invasion and Inactivating Extracellular Merozoites

Authors

Greta E. Weiss[1], Robert J. Ragotte[2], Doris Quinkert[2,3], Amelia M. Lias[2,3], Madeline G. Dans[1], Coralie Boulet[1], Barnabas G. Williams[2,3], Brendan S. Crabb[1,4], Simon J. Draper[2,3], and Paul R. Gilson[1,4#].

Affiliations

[1]Burnet Institute, 85 Commercial Road, Melbourne, Victoria 3004, Australia

[2]Department of Biochemistry, University of Oxford, Dorothy Crowfoot Hodgkin Building, Oxford, OX1 3QU, United Kingdom

[3]Kavli Institute for Nanoscience Discovery, University of Oxford, Dorothy Crowfoot Hodgkin Building, Oxford, OX1 3QU, United Kingdom.

[4]The University of Melbourne, Grattan Street, Parkville, Victoria 3010, Australia

Corresponding author

Keywords

18 Plasmodium falciparum, invasion, merozoites, vaccines, monoclonal antibodies, reticulocyte-
19 binding protein homolog 5.

Abstract

The *Plasmodium falciparum* reticulocyte-binding protein homolog 5 (PfRH5) is the current leading blood-stage malaria vaccine candidate. PfRH5 functions as part of the pentameric PCRCR complex containing PTRAMP, CSS, PfCyRPA and PfRIPR, all of which are essential for infection of human red blood cells (RBCs). To trigger RBC invasion, PfRH5 engages with RBC protein basigin in a step termed the RH5-basigin binding stage. Although we know increasingly more about how antibodies specific for PfRH5 can block invasion, much less is known about how antibodies recognizing other members of the PCRCR complex can inhibit invasion. To address this, we performed live cell imaging using monoclonal antibodies (mAbs) which bind PfRH5 and PfCyRPA. We measured the degree and timing of the invasion inhibition, the stage at which it occurred, as well as subsequent events. We show that parasite invasion is blocked by individual mAbs, and the degree of inhibition is enhanced when combining a mAb specific for PfRH5 with one binding PfCyRPA. In addition to directly establishing the invasion-blocking capacity of the mAbs, we identified a secondary action of certain mAbs on extracellular parasites that had not yet invaded where the mAbs appeared to inactivate the parasites by triggering a developmental pathway normally only seen after successful invasion. These findings suggest that epitopes within the PfCyRPA-PfRH5 sub-complex that elicit these dual responses may be more effective immunogens than neighboring epitopes by both blocking parasites from invading and rapidly inactivating extracellular parasites. These two protective mechanisms, prevention of invasion and inactivation of uninvaded parasites, resulting from antibody to a single epitope indicate a possible route to the development of more effective vaccines.

Author Summary

Malaria is a sometimes-fatal disease caused by protozoan parasites of which *Plasmodium falciparum* is the most deadly species that causes hundreds of millions of infections and half a million deaths per year. A partially effective vaccine is available to block parasite forms transmitted by mosquitoes but not the subsequent blood stage which causes symptomatic disease. To fight blood stage parasites, proteins have been identified such as PfRH5, that aid parasite entry into human red blood cells (RBCs) and vaccines made from these proteins can trigger the production of antibodies that bind the parasite proteins thereby blocking RBC invasion. PfRH5 forms a complex with another parasite protein called PfCyRPA and together antibodies to PfCyRPA and PfRH5 are highly effective in reducing parasite growth. Here we investigated how antibodies to PfCyRPA and PfRH5 actually block invasion using video microscopy of live parasites. As anticipated, we found the antibodies not only stopped most parasites from invading but of those parasites that did invade, they took longer to do so, suggesting the antibodies were physically inhibiting the invasion process. One unanticipated effect of both PfRH5 antibodies and one of three PfCyRPA antibodies tested, was that they triggered the uninvaded parasites to change into cellular forms normally only seen inside RBCs. These intracellular forms are no longer competent to invade and so the PfRH5/CyRPA antibodies have the potential of both neutralize parasites by physically preventing RBC entry and by changing the parasites into invasion incompetent forms.

Introduction

Globally, malaria remains a serious problem with 247 million cases of malaria worldwide, and 619,000 deaths in 2021 [1], with the majority of disease burden and death due to *Plasmodium falciparum* (*Pf*). Despite a growing arsenal of antimalarial drugs, it is unlikely that drugs alone will be enough to eradicate malaria. Disruptions to pharmaceutical supply chains caused an increase in malaria disease burden during the COVID-19 pandemic, further underlining the importance of a highly effective malaria vaccine, which would continue to provide protection when medicines are not available, or when a constant medical presence is not possible.

Antibodies are known to play a key role in protection from malaria [2]. Low-level antibody responses to parasite invasion protein PfRH5, can be naturally-acquired following many years of malaria exposure and associate with clinical immunity and inhibit parasite growth *in-vitro* [3]. High levels of PfRH5 vaccine-induced antibodies can block merozoite invasion of erythrocytes [4], and are associated with delayed time to diagnosis in a controlled human malaria infection trial in vaccinated individuals [5]. PfRH5 forms a chain-like PCRCR complex with *P. falciparum* Cysteine-Rich Protective Antigen (PfCyRPA), PfRH5-interacting protein (PfRIPR), *P. falciparum* cysteine-rich small secreted protein (PfCSS) and *P. falciparum* Plasmodium thrombospondin-related apical merozoite protein (PfPTRAMP) [6-8], which has been shown to localize at the tight junction between the merozoite and erythrocyte immediately prior to invasion [6, 9]. PfRH5, PfCyRPA, PfRIPR, PfCSS and PfPTRAMP are required for merozoite invasion of erythrocytes with PfRH5, PfCyRPA, PfRIPR each able to stimulate the production of cross-strain neutralizing antibodies [6, 9-15]. Of the five PCRCR components, PfRH5, PfCyRPA and PfRIPR are the most well

84 characterized and are compelling malaria vaccine candidates with experimental vaccination of
85 non-human primates and humans with PfRH5 producing potent neutralizing antibodies [16, 17].
86 Understanding the effect of antibodies targeting the PCRCR complex antigens, both in isolation
87 and combination, is now critical to effective next-generation blood-stage vaccine design.
88 Importantly, the amount of antibody required for protection may be greatly reduced by
89 exploiting synergistic interactions between antibodies.

90 Antibodies recognizing the same complex could be expected to synergize through a wide variety
91 of mechanisms, including, but not limited to, causing a conformational change that enhances
92 binding of a second antibody [18] slowing down invasive processes allowing other antibodies
93 more time to bind [4] or by stabilizing antibody binding through lateral interactions [19]. The
94 ideal effect of antibodies would be rapid and lead to permanent disabling of the parasites' ability
95 to invade or survive. While antibody binding to a parasite might temporarily prevent invasion, if
96 that parasite is not disabled by this interaction, then the dissociation of that antibody could leave
97 the parasite virulent and able to attempt invasion again.

98 In this study we use live cell imaging to examine the visible temporal and morphological effects
99 of mAbs binding to different epitopes of PfRH5 and PfCyRPA on invasion, the post-invasion
100 development of young parasites, and the inactivation of uninvaded merozoites. While the ability
101 of PCRCR antigen-specific antibodies to block invasion is known, this is the first report of their
102 capacity to inactivate uninvaded parasites. This work illuminates new mechanisms through
103 which neutralizing antibodies to certain epitopes of PfRH5 and PfCyRPA function and future

104 studies of the cellular and molecular basis of these observations could open the door to strategies
105 for the rational design of a highly effective blood-stage malaria vaccine.

106 ## Results

107 ### Antibody inhibition of merozoite invasion

108 To characterize the effects of mAbs specific for PfRH5 and PfCyRPA on invasion of erythrocytes,
109 live cell microscopy was performed on clonal 3D7 parasites using methods that had been
110 previously developed [20]. As expected, parasites in the presence of the control EBL 040 mAb
111 (targeting *Ebola virus*)[4, 21] followed the usual progression of invasion with distinct stages
112 marked first by egress of merozoites from the schizont (Fig 1A, S1 Table, S1 Video) [20, 22, 23],
113 contact of the merozoite with the erythrocyte, and deformation of the erythrocyte membrane.
114 Following this is the short stage where the PCRCR complex acts and the tight junction forms
115 between the merozoite and erythrocyte. Here we term this the “RH5-basigin binding stage”, and
116 merozoite invasion of the erythrocyte ensues over the next 10 seconds. After this, temporary
117 changes to the invaded erythrocyte occur called echinocytosis, and the merozoite differentiates
118 into an intracellular ring (Fig 1A, S1 Video).

119 Anti-PfRH5 mAbs were isolated from volunteers immunized in the first human Phase Ia PfRH5
120 vaccine trial [24]. Individual mAbs were characterized: clone R5.004 was found to be strongly
121 neutralizing and to bind directly to the basigin-binding site of PfRH5 [4]; whilst clone R5.008 was
122 found to be moderately neutralizing possibly by hindering PfRH5’s access to basigin through
123 steric clashes with the RBC membrane or basigin’s RBC binding partners PCMA or MCT1 (S1 Fig A

and B) [4, 25]. It has recently been discovered that PfRH5 must have its pro-sequence cleaved by plasmepsin X before it can engage basigin [26].

We also analyzed three mAbs which bind PfCyRPA and were composed of variable regions from vaccinated chickens and a human IgG1 constant region [19]. These three mAbs all bind to the beta propeller blade 1 and 2 regions of PfCyRPA (S1 Fig C and D). PfCyRPA-binding mAbs demonstrated modest levels of inhibition [7]. However, in growth inhibition activity (GIA) assays, R5.008 and Cy.009 synergized to strongly inhibit invasion (Fig 1B). Because of this, R5.008 was filmed at a concentration causing less inhibition to directly compare results with the R5.008 + Cy.009 combination, while other individual mAbs were filmed at concentrations resulting in an intermediate level of inhibition to assess the stages of invasion that were affected. We also evaluated PfCyRPA fragment antigen binding (Fab) molecules in GIA assays and found the Fabs consistently demonstrated greater GIA than whole IgGs at equivalent molarities (Fig 1C, S1 Fig E-G). Since this was especially evident for Cy.007, with Fabs being about >10-fold more inhibitory than whole IgGs, we included this Fab in our live imaging analysis.

Videos of egress and invasion were analyzed in detail for each of the mAbs, Fabs and the control EBL 040 antibody with a median of 11 videos analyzed for each antibody. The concentration used are indicated in brackets (in µg/mL). The number of merozoite-erythrocyte contacts per egress was noted and was equal to or greater than that in the control antibody, indicating the parasites were healthy (Fig 2A, S2A Table). In addition, the times from egress to first merozoite contact with erythrocytes were similar demonstrating the experimental conditions were consistent for each antibody combination (Fig S2A, S5A Table). With the exception of R5.004-(22) the antibodies

did not greatly reduce the degree with which the merozoites deformed their target RBCs which is thought to be a product of merozoite ligands acting upstream of the PCRCR complex and the actomyosin invasion motor (S2B Fig, S5B Table) [20].

The number of invasions per egress was reduced in the R5.004-(22), Cy.003-(250) and Cy.007 antibodies as well as in the R5.008-(40) + Cy.009-(200) combination as compared to the control EBL 040-(400) (Fig 2B, S2B Table, S1-S10 Videos). As the direction of schizont egress and the number of erythrocytes available for invasion can vary, a complementary measure of invasion was also used: the percentage of merozoites that invade after contacting an erythrocyte. Using this measure, invasion was reduced for all anti-PfRH5 and -PfCyRPA antibodies compared to the control (Fig 2C, S2C Table). R5.004-(22), Cy.007 Fab-(133) and -(400), and the combination of R5.008-(40) + Cy.009-(200) were so inhibitory, at 97.5-100% inhibition, that these yielded limited data (Fig 2C). In three experimental conditions, R5.008-(40), Cy.003-(250) and Cy.007-(400), some merozoites regressed back out of the erythrocyte a short time after invasion, which we have referred to as “regression” (Fig 2D, S2D Table). To account for this we assessed “productive invasions” which are those invasions where the merozoite remains inside the erythrocyte during the 20-minute observation period (Fig 2E). Overall, the number of productive invasions per egress and the percentage of productive invasions per contact showed similar trends to the total numbers of invasions per egress and percentage of invasions per contact (Fig 2B versus 2E and Fig 2C versus 2F, S2E-F Table).

Importantly, for R5.004(22), Cy.009(200), Cy.003(250) and Cy.007(400) there were no statistically significant differences when comparing the number of invasions per egress, productive invasions

per egress, or the percent of contacts which invaded or resulted in productive invasions (Fig 2, S2 Tables). This allowed us to proceed comparing the different mechanisms of invasion inhibition which occur with these various mAbs, given the overall level of invasion inhibition is comparable whilst the invasion stages affected by the mAbs could vary.

Antibody effects on early pre-invasion interactions

Pre-invasion consists of the time from first contact between the erythrocyte and merozoite to the start of invasion, with early pre-invasion events including initial contact and erythrocyte deformation (Fig 1A). The antibodies did not greatly change the short period of time from first merozoite contact to the start of erythrocyte deformation, although R5.004-(22) was slightly shortened relative to Cy.009-(200) and Cy.007-(400) (Fig 3A, S3A Table). R5.004-(22) also shortened the duration of deformation (mean 8.3 s) compared to PfCyRPA-binding mAbs (Fig 3B, S3B Table). Although Cy.007-(400) prolonged deformation (mean: 107.9 s) compared to R5.004-(22), R5.008-(40) and Cy.009-(200), this was not significantly different to EBL 040 control (mean: 52.7 s) (Fig 3B, S3B Table). The CyRPA-binding mAb Cy.007-(400) prolonged the whole pre-invasion period from first contact to the start of invasion in comparison to the control antibody, RH5-binding mAbs and Cy.009-(60) and Cy.003-(250) (Fig 3C, S3C Table).

Antibody effects on the complex stage; late pre-invasion interactions

The RH5-basigin binding stage, the time from the end of deformation to the start of invasion, is the time PCRCR is thought to have its primary function, aiding rhoptry release and tight junction formation [6, 9, 20]. This stage of invasion is tightly regulated, with an average time of 1.8 to 2.0

s (Fig 1A, S1 Table) [20]. In comparison to control antibody EBL 040, both R5.004-(22) and R5.008-(40), as well as Cy.009-(60 and 200) caused a delay at this stage, that was dose dependent in the case of Cy.009 (Fig 3D, S3D Table). Although there was only a single instance of an invasion under these conditions, the R5.008-(40) + Cy.009-(200) combination resulted in the longest delay, which at 17.75 s was slightly longer than the sum of the means of each antibody alone (14.27 s). In contrast, the PfCyRPA-binding Cy.003-(250) and Cy.007 antibodies did not cause a delay at this stage of invasion (Fig 3D).

Antibody effects on invasion

Internalization of the parasite, measured from the time the merozoite begins to enter the erythrocyte until it is entirely inside the erythrocyte, typically has little variability and consistently takes about 10 s (Fig 1A, S1 Table) [20]. The Cy.003-(250) and Cy.007-(400) significantly slowed internalization, causing this stage to take approximately double the time observed in the presence of control antibody or the other individual antibodies (Fig 3E, S3E Table). Although R5.008-(40) and Cy.009-(60) decreased the time of internalization, the combination of these two antibodies greatly slowed the invasion time, although this combination was so inhibitory there was only a single invasion observed (Fig 3E). When the RH5-basigin binding stage and invasion stages were combined there was an overall increase in the time from the end of deformation to the end of invasion for R5.004-(22), Cy.009-(200), Cy.003-(250) and Cy.007-(400) compared to the control (S2C Fig, S5C Table).

Antibody effects on echinocytosis

After invasion is completed, the invaded erythrocyte typically becomes spherical with distinctive spikes covering its surface for several minutes before returning to its usual biconcave shape [22, 23] (Fig 1A). This process is called echinocytosis and is strongly associated with successful invasions [20]. We noted that there were significant reductions in the numbers of these events per egress for the R5.008 and Cy.009 combination as well as the Cy.007 Fabs and IgGs (Fig 3F and S3F Table) like the invasions per egress data (Fig 2B). The echinocytosis stage of the invasion process has wide natural variability spanning several minutes. For every individual mAb, there were instances of echinocytosis starting before invasion had completed, something rarely observed previously [20, 27] (negative values in Fig 3G and S3G Table). Echinocytosis was triggered earlier for parasites in the presence of R5.008-(40) (mean 15.0 s) and Cy.009-(60 and 200) (mean 18.00 and 3.8 s, respectively) compared to EBL 040 (mean 40.9 s)(Fig 3G and S3G Table). Since PfRH5 likely binds basigin at the end of deformation [20], and PCRCR-complex binding has been linked to echinocytosis [27], we examined this time period (end of deformation to start of echinocytosis). R5.008-(40) and Cy.009-(60) caused a decrease in this time (Fig 3H and S3H Table). Although the CyRPA antibodies tended to increase the mean duration of echinocytosis this was only statistically significant for Cy.003-(250) (S2D Fig and S5D Table).

To further analyze echinocytosis of the newly invaded RBCs, we measured increasing echinocytosis, the time from the initiation of echinocytosis to the point when maximum echinocytosis was reached, the duration of maximum echinocytosis, and decreasing echinocytosis, the time it took for the erythrocyte to recover its usual biconcave shape (Fig 1A, S1 Table). For the EBL 040 control, increasing echinocytosis lasted a mean of 42.0 s, maximum

echinocytosis 395.9 s, and decreasing echinocytosis 615.8 s (S2E-G Fig, S1 Table, S5E-H Table). The mean time required for increasing echinocytosis was highly variable for Cy.003-(250) and Cy.007-(400) but this only reached significance for Cy.007-(400) (mean 98.2 s) which was more than double that of the control (mean 44.2 s)(S2E Fig and S5E Table). Similarly for the duration of maximum echinocytosis, Cy.007-(400) was highly variable but not significantly so compared to the control (S2F Fig and S5F Table). For the period of decreasing echinocyotsis, the mean duration for R5.008-(40), Cy.009-(200), Cy.003-(250) and Cy.007-(400) increased relative to the control but was only statistically significant for Cy.003-(250) (S2G Fig and S5G Table). Despite echinocytosis being a post invasion phenomenon, the antibodies that targeted PfRH5 and PfCyRPA were able to exert an inhibitory/delaying/slowing effect, particularly for Cy.007-(400). Echinocytosis is thought to be triggered by RBC membrane lipid perturbations caused during merozoite invasion: the invasion slowing effects of the antibodies may have increased these effects thereby extending the period of echinocytosis [20, 27].

Overall order and morphology of normal early ring development

We next examined the potential effects of the PfRH5 and PfCyRPA antibodies on the differentiation of merozoites into ring-stage parasites. Current knowledge of new ring development is largely restricted to observations of merozoites spinning or oscillating immediately following invasion in *P. knowlesi* and *P. falciparum* [22, 27], with the most detailed description of the stages from an electron microscopy study on *P. knowlesi* [28]. Before examining the effects of PfRH5 and PfCyRPA antibodies we first performed live cell imaging on parasites treated with the control EBL 040-(400) and found that the intraerythrocytic merozoites

begin to spin on average 16.4 s after the completion of invasion (Fig 1A). The spinning lasted an average of 116.3 s followed by the growth of a pseudopod like protrusion from the merozoite 159.2 s later. Almost a minute later (av. 57.2 s), the merozoite lost its rounded shape and became irregular and was defined as a “preliminary ring” (Fig 1A, S1 Table). Almost 10 minutes after this (av. 638 s) a fully amoeboid ring was formed, defined as the point at which all dense regions on the rings became fluid and mobile (Fig 1A, S1 Table).

In the presence of EBL 040-(400), early ring development occurred in nearly all merozoites which invaded and became intracellular, with 97.4% forming a pseudopod-like protrusion (Fig 4A, S4A Table). Of the original invaders, 88.3% continued differentiation into preliminary rings (Fig 4B, S4B Table) and 70% developed into amoeboid rings during the 20-minute observation period (Fig 4C, S4C Table). During this time, the parasites remained at the invasion site and were likely tethered to the erythrocyte surface with no occurrences of fission between the parasitophorous vacuole membrane and erythrocyte membrane.

Most uninvaded, extracellular merozoites in the presence of EBL 040 IgG appeared unchanged over the 20-minute observation period. However, some extracellular merozoites began to spin with 10.7% of the original extracellular merozoites eventually developing pseudopods. Following this, 7.5% of the EBL 040 IgG treated merozoites lost their typically rounded shape and became more irregular. These so-called ‘preliminary rings’ then became fully amoeboid forms with 2.8% of the original EBL 040 IgG treated merozoites becoming amoebas (Fig 4A-C; S4A-C Table). As the pseudopods of the extracellular amoeba were not restrained within a parasitophorous vacuole, they became greatly elongated.

Antibody mediated inactivation of extracellular merozoites

In the presence of anti-PfRH5 and -PfCyRPA mAbs, the percentage of merozoites beginning to differentiate into intracellular rings by developing pseudopods after invasion was very high and comparable to the control (Fig 4A, S4A Table). The percentages of merozoites that differentiated into intracellular preliminary rings and into complete rings in the presence of these mAbs was likewise similar to the EBL 040 control (Fig 4B and C and S4B and C Tables). A major difference was observed, however, for extracellular merozoites in R5.004-(22), R5.004-(200), R5.008-(40), Cy.009-(60) and Cy.009-(200), where most of the merozoites began to differentiate into rings by growing pseudopods compared to EBL 040, Cy.003-(250) and Cy.007 conditions (Fig 4A and D, S4A Tables, S1-S6 Videos). Extracellular merozoites developed pseudopods in 97.8% of cases in R5.004-(22), 99.5% in R5.004-(200), 96.7% in R5.008-(40), 71.1% in Cy.009-(200) and 100% of cases in the R5.008-(40)+Cy.009-(200) combination (Fig 4A, S4A Table, S2-S6 Videos). Following on, most of the PfRH5 and Cy.009 mAb treated extracellular merozoites developed into preliminary rings as they lost their rounded shape which reached 96.5% in R5.004-(22), 99.5% in R5.004-(200), 70.0% in R5.008-(40), 69.8% in Cy.009-(200) and 100% in the R5.008-(40)+Cy.009-(200) combination (Fig 4B, S4B Table, S2-S6 Videos).

The extracellular preliminary rings then differentiated into fully amoeboid rings in 89.0% of cases in R5.004-(22), 96.7% in R5.004-(200), 31.7% in R5.008-(40), 56.4% in Cy.009-(200) and 95.6% of cases in the R5.008-(40)+Cy.009-(200) combination (Fig 4C, S4C Table). The percentage of extracellular merozoites in R5.004-(22) and R5.008-(40), R5.004-(200) and the R5.008-

289 (40)+Cy.009-(200) combination which develop into extracellular rings is comparable to invaded
290 merozoites at every stage of ring development (Fig 4A-D, S4A-C Table).

291 In contrast, Cy.003, Cy.007 Fab, and Cy.007 IgG caused no additional extracellular ring
292 development compared to the EBL 040 control (Fig 4A-D, S4A-C Tables, S7-S10 Videos). Cy.007
293 Fab-(400) was noteworthy as no extracellular merozoites reached the amoeboid ring stage (Fig
294 4C). While most conditions caused either nearly complete or close to no extracellular ring
295 development, Cy.009-(60) caused intermediate levels of extracellular pseudopod (41.4%),
296 preliminary ring (36.9%), and amoeboid ring (24.2%) development, leaving this group differing
297 from the binary situation evident with other conditions (Fig 4A-D, S4A-C Tables).

298 **Antibody effects on regression**

299 As mentioned previously, in the presence of R5.008-(40), Cy.003-(250), and Cy.007-(400), some
300 merozoites regressed out of erythrocytes after invasion compared to no regression in EBL 040
301 (Fig 2D). Specifically, 22.78% of R5.008-(40) invasions regressed, 19.00% in Cy.003-(250) and
302 33.33% in Cy007-(400) (Figs 2D, S2D Table; S1, S3, S7 and S11 Video). We observed that most
303 regressed merozoites became fully differentiated extracellular rings within the 20-minute
304 observation (Fig 4A-C, S4A-C Table).

305 **Antibody effects on merozoite spinning**

306 As indicated in Fig 1A, the first notable activity performed by merozoites after invasion is their
307 spinning, oscillating, or twisting actions that have been implicated in helping sever the nascent

PVM from the host cell plasma membrane [22, 27, 29]. To compare extracellular and intracellular ring development, we measured time from egress (when merozoite exposure to mAbs began) to the start of spinning (the first observable indication of ring conversion). On average, in the presence of EBL 040, intracellular merozoites began spinning 173.5 s after egress, more quickly than extracellular merozoites at 284.1 s (S3A Fig, S6A Table). Here, intracellular merozoites spun for nearly two minutes and extracellular merozoites for nearly 4 minutes (S3B, S6B Table). As a general observation, the mean times from egress to spinning for extracellular merozoites were shorter in the presence of the anti-PfRH5 mAbs than the extracellular control but this only reached significance for the R5.004 mAbs (Fig S3A, S6A Table). The times to spinning for the same extracellular anti-PfRH5 mAb treated merozoites were similar to the invaded intracellular EBL 040 treated merozoites (mean 173.5 s) with the exception of R5.004-(22) which could start spinning in as little as 21 s (mean 88 s, Fig S3A, S6A Table).

The duration of spinning in all extracellular merozoites developing into rings was comparable to that observed in intracellular EBL 040 except for parasites in R5.004-(200) and Cy.009-(200) which spun for less time and Cy.007-(400) where spinning lasted longer (S3B Fig, S6B Table). For extracellular merozoites in the presence of R5.004-(22), R5.004-(200) and Cy.009-(200), the duration of spinning was shorter than in the extracellular EBL 040 control (S3B Fig, S6B Table).

Antibody effects on pseudopod formation

R5.004, R5.008-(40), and Cy.009 treated intracellular merozoites usually stopped spinning before the pseudopod became visible, similar to both EBL040 controls producing positive values (S3C

Fig, S6C Table). In contrast, pseudopods were often visible before the end of spinning of intracellular merozoites in most Cy.003 and Cy.007 events, producing negative values (S3C Fig, S6C Table). For most of the antibody-treated extracellular merozoites, the first pseudopod was often visible before the end of spinning compared to intracellular merozoites. This was particularly so for extracellular merozoites treated with Cy.003 or Cy.007 suggesting merozoite development may be more dysregulated for extracellular compared to intracellular merozoites (S3C Fig).

Antibody effects on preliminary ring formation

For intracellular merozoites, preliminary ring formation was defined as the time from the merozoite's pseudopod first being visible until disruption of the rest of the merozoite's plasma membrane (Fig 1A). For most intracellular merozoites in the presence of anti-PfRh5 and -PfCyRPA mAbs, the time to preliminary ring formation was comparable to the control antibody except for Cy.003 which took 4.5-fold longer (S3D Fig, S6D Table). For extracellular merozoites exposed to R5.004, R5.008 and Cy.009, it took less time for the merozoites to become preliminary rings than the extracellular EBA 040 control marked from when the first pseudopod was visible to when the merozoite became more irregularly shaped. In R5.004, R5.008 and Cy.009 IgGs, the extracellular merozoites became preliminary rings with similar times as the intracellular EBA 040 control (S3D Fig, S6D Table). For extracellular Cy.003 merozoites, preliminary development again took 4-fold longer than extracellular and intracellular controls (S3D Fig, S6D Table).

Antibody effects on amoeboid ring formation

For PfRH5 and PfCyRPA antibody-treated intracellular parasites, the time from merozoite membrane disruption to complete ring formation was similar to the intracellular EBA 040 control (S3E Fig, S6E Table). Extracellular merozoites in the presence of R5.004-(200) took less time to develop into amoeboid rings than the extracellular control (S3E Fig). Our observations generally indicated that anti-PfRH5-exposed extracellular merozoites, which are efficiently neutralized and converted to ring-like forms, do so in similar stages and timings as merozoites which have successfully invaded. In contrast, the Cy.003 and Cy.007 treated merozoites both intracellular and extracellular tend to be more dysregulated often taking longer to complete the neutralization steps. Finally, in the presence of R5.008-(40), timing of regressed merozoite differentiation was comparable to that of successful invasions, while regressed Cy.003-(250) and Cy007-(400) merozoites had timing similar to that of extracellular merozoite differentiation (S3D and E Fig, S6D and E Table).

Discussion

Live cell invasion imaging has previously played an important role in establishing how the invasion slowing anti-PfRH5 human mAb R5.011 could boost the potency of the invasion-neutralizing human mAb R5.016 [4]. Indeed, these data identified a mechanism of synergy between non-competing vaccine-induced antibody clones that bound different epitopes on PfRH5 [4]. We thus decided to apply this approach to study potential synergies between anti-PfRH5 and -PfCyRPA antibodies. We discovered that anti-PfRH5 mAbs generally appear to slow aspects of the pre-

368 invasion complex phase during which the tight junction formed, while anti-PfCyRPA mAbs appear
369 to slow the initial deformation stage and the downstream internalization stage where the
370 merozoite penetrates its erythrocyte. An exception was Cy.009 which often behaved more like
371 an anti-PfRH5 mAb rather than the other anti-PfCyRPA mAbs. Titration of R5.008 alone and in
372 combination with Cy.009 indicated this anti-PfCyRPA mAb was able to synergistically boost the
373 inhibitory capacity of R5.008 both in GIA assays and by live cell imaging. Hopefully these synergies
374 can be clinically achieved considering recent experimental vaccinations of rats with PfRH5 and
375 PfCyRPA antigens combinations did not produce IgGs that inhibited *in vitro* parasite growth much
376 better than PfRH5 antigen antibody alone [30].

377 We also observed for the first time that PfRH5 and Cy.009 antibodies have effects on the post-
378 invasion period (where newly invaded intraerythrocytic merozoites differentiate into ring-stage
379 parasites). Unexpectedly, we found that the anti-PfRH5 mAbs and Cy.009 caused most of the
380 merozoites that had not invaded to rapidly differentiate into amoeboid forms, which we believe
381 are equivalent to ring-stage parasites. It is anticipated that the rapid induction of extracellular
382 merozoites into rings could block the capacity of the parasites to attempt re-invasion and could
383 increase the potency of antibodies that target PfRH5 and PfCyRPA.

384 One of the most inhibitory anti-PfRH5 human mAbs reported is R5.004 [4], which binds directly
385 to the basigin binding site of PfRH5. R5.008 binds near the basigin binding site of PfRH5, probably
386 sterically hindering PfRH5's access to basigin. Using several measures, both PfRH5 mAbs reduced
387 the number of invasions (per egress and invasions per merozoite-erythrocyte contact). This also
388 applied to productive invasions where the merozoites did not regress during the observation

389 period. For the limited number of invasions that were successful, our live cell imaging indicated
390 both mAbs caused significant delay between the end of deformation and the start of
391 internalization when PfRH5 is thought to bind basigin as part of the PCRCR complex [6, 8, 9, 20].
392 It therefore seems likely that during erythrocyte contact, there is competition between basigin
393 and the anti-PfRH5 mAbs to gain access to PfRH5 with a threshold level of interaction between
394 PfRH5 and basigin required for successful invasion. Competition between basigin and the anti-
395 PfRH5 mAbs for PfRH5 likely delays time to reach the invasion threshold.

396 The anti-PfCyRPA mAbs were also very potent at inhibiting invasion using the invasions per egress
397 and invasions per contact measurements with the Cy.007 Fabs being especially effective. This
398 indicates that the Cy.007 Fab may be able to access its epitope far more effectively in the
399 confined space between the merozoite apex and the RBC bound basigin complex [25] than the
400 whole 150 kDa IgG even though the Fab would have less avidity than parental mAb. Of the
401 invasions which did occur, Cy.009 behaved (in a dose-dependent manner) similarly to the anti-
402 PfRH5 mAbs by delaying the start of invasion after the end of deformation, suggesting Cy.009
403 may inhibit PCRCR complex formation or the binding of PCRCR to basigin [4, 6]. Although Cy.009
404 does not occupy basigin's binding site on PfRH5 it could sterically inhibit PfRH5 from binding to
405 basigin, particularly in the crowded environment at the erythrocyte membrane where basigin
406 binds RBC partner proteins PCMA or MCT1 [8, 25]. Cy.003 and Cy.007 on the other hand did not
407 delay PCRCR complex formation or the binding of PCRCR to basigin but rather slowed down
408 merozoite internalization. This could be due to the mAbs somehow slowing movement of the
409 merozoite through the tight junction into the erythrocyte. The combination of the R5.008 and

Cy.009 mAbs so greatly inhibited invasion that only one event was recorded. Here, Cy.009 appeared to function similarly to the potentiating mAb R5.011, in that it slowed the pre-invasion phase allowing more time for the neutralizing PfRH5 mAb to function [4]. Although Cy.009 did not appear to increase pre-invasion times as much as R5.011 [4], Cy.009 was much more inhibitory by itself and proved particularly effective in combination with R5.008. How mAb-induced interference of the PCRCR complex mechanistically blocks invasion will be explored later during the discussion of extracellular differentiation into rings.

Once merozoite internalization is complete, the erythrocyte starts to become an echinocyte about half a minute later. This is thought to be due to the deposition of lipids and other materials from the parasite rhoptries into the erythrocyte membrane causing asymmetry in the lipid bilayer, producing outward bending protrusions of the erythrocyte surface [20, 27]. Recently, high resolution lattice light sheet microscopy has revealed that echinocytosis probably begins much sooner after invasion than previously thought, evident as undulations of the erythrocyte membrane [27]. We concur that the time it takes for echinocytosis to reach its maximum and for the erythrocyte to return to its normal biconcave shape vary broadly [20, 27]. The only consistently observed effect of the antibodies upon echinocytosis was that it appeared to initiate more rapidly during treatment with the anti-PfRH5 and Cy.009 mAbs after invasion, possibly because invasion had been delayed.

The transformation of newly invaded merozoites into ring-stage parasites was described several decades ago for *P. knowlesi* with the characteristic steps of merozoite spinning, pseudopod growth and transformation of the circular shaped merozoite into an amoeboid ring [22, 28]. Here

we examined the timing of these events in *P. falciparum* and found the conversion steps were conserved and that most invaded merozoites converted into rings. Spinning or oscillation of newly invaded *P. falciparum* merozoites have been previously noted and are thought to be a mechanical mechanism to promote severance of the parasitophorous vacuole membrane from the host cell membrane [27, 29]. Although we know little about merozoite spinning and the various downstream steps that result in conversion into rings, it is interesting that anti-PfRH5 and -PfCyRPA antibodies, particularly Cy.003 and Cy.007, could still influence ring differentiation (*e.g.,* increasing spinning duration) despite the merozoites having already invaded. Whether the antibodies ultimately reduce the successful transformation and growth of intraerythrocytic parasites is not yet known.

The most interesting phenomenon observed in the presence of the antibodies was the rapid transformation of extracellular merozoites into amoeboid forms we believe are equivalent to intraerythrocytic rings. This was most evident in the presence of anti-PfRH5 mAbs and Cy.009, where 50-100% of extracellular merozoites became rings compared to around 10% in the presence of the EBL 040 control IgG and the other anti-PfCyRPA mAbs. In the presence of anti-PfRH5 mAbs, Cy.009, and the R5.008 + Cy.009 combination, the time from merozoite egress and hence antibody exposure, to transformation into extracellular rings occurred with similar timing as successfully invaded merozoites. Extracellular ring development is particularly interesting because it would presumably inactivate and neutralize the extracellular merozoites, preventing them from attempting another round of invasion. As egressed merozoites have been estimated

to have a half-life of 5 minutes, this could mean a substantial proportion of the extracellular merozoites could be inactivated while they are still invasion competent [31].

The mechanism by which the anti-PfRH5 and Cy.009 antibodies trigger ring development in extracellular merozoites is not yet understood but we believe that induction is potentially mimicking some naturally occurring step that takes place during normal invasion. It has been shown that the PCRCR complex and basigin are involved in triggering a calcium ion flux event at the apical end of merozoites that are about to invade erythrocytes [9, 20, 27]. This event is thought to be part of tight junction formation whereby the rhoptries and micronemes release proteins that form the ring-like junction with the erythrocyte surface through which the merozoite propels itself into the erythrocyte [9, 20, 32-34]. It is possible that binding of IgGs to PfRH5 and subsequent crosslinking mediated by the bivalent IgG molecules may mimic binding of PfRH5 with basigin at the erythrocyte surface and trigger a merozoite apical calcium ion flux that initiates a signaling cascade in the merozoite leading to ring development. Experiments with merozoites treated with fluorescent calcium dyes could help resolve if the PfRH5 mAbs are triggering apical calcium fluxes.

It is curious that the Cy.009 antibody also promotes extracellular merozoite ring development given the Cy.003 and Cy.007 are not any more effective than EBL 040 control. Cy.009 binds to the B1 and B2 propeller regions of PfCyRPA like the other PfCyRPA mAbs, so perhaps subtle differences in its angle of binding are responsible for Cy.009's ring promoting activity [7]. It is therefore important to understand the fine specificity of the anti-PfCyRPA mAbs for their

471 epitopes because even though they bind to same PfCyRPA blades, the epitopes do not overlap,
472 and this could have important biological implications as observed here.

473

474 ## Conclusions

475 Here we have demonstrated that antibodies to PfRH5 and PfCyRPA block merozoite invasion and
476 that mAbs R5.008 and Cy.009, that are specific for each of these respective proteins, function
477 synergistically. Live cell imaging in the presence of antibodies at concentrations that partly
478 reduce invasion indicate that the anti-PfRH5 and Cy.009 mAbs increase the period of PfRH5-
479 basigin invasion complex formation suggesting they might reduce the efficiency with which
480 PfRH5 can functionally access basigin. The other anti-PfCyRPA mAbs increase the time taken for
481 merozoites to internalize, suggesting they could sterically inhibit the speed with which the
482 merozoite passes through the tight junction which could indicate the PCRCR complex still persists
483 at the tight junction during invasion. The mAbs also influence speed and efficiency with which
484 invaded merozoites can differentiate into intraerythrocytic ring-stage parasites which is
485 surprising as the PCRCR complex functions well before this. The most unexpected finding was
486 that anti-PfRH5 and Cy.009 mAbs trigger rapid differentiation of extracellular uninvaded
487 merozoites into ring-like parasites. We next aim to determine if the differentiation of invasion
488 competent merozoites into invasion-incapable extracellular rings is rapid enough and occurs at
489 antibody concentrations low enough to majorly boost the protective immunity of PfRH5 and
490 PfCyRPA antigen-based human vaccines and how this can be improved.

Materials and Methods

Growth Inhibition Activity Assays

Growth Inhibition activity (GIA) assays were performed to the protocol of the international GIA reference center at NIAID, NIH, USA [35]. Parasite cultures were synchronized using treatment with 5% sorbitol on the day before GIA assay set up. One-cycle GIA assays were performed at the indicated concentrations of mAbs. Biochemical measurement using a *P. falciparum* lactate dehydrogenase assay was used to quantify endpoint parasitemia which has been described previously [36] Percent GIA was calculated using the following equation where RBC are red blood cells:

$$\% \text{ GIA} = 100 - 100 * (A650_{\text{sample}} - A650_{\text{uninfected RBC}}) / (A650_{\text{infected control}} - A650_{\text{uninfected RBC}})$$

Assays were quality-controlled by inclusion of the anti-PfRH5 mAb 2AC7 as an in-plate control, and the anti-PfRH5 mAbs 2AC7, QA5, 9AD4 as external plate controls [37]. 5 mM EDTA is included as a positive control and a Zaire Ebolavirus glycoprotein-67 reactive IgG1 mAb (EBL 040) [21] was used as a negative isotype control for mAb samples.

To assess synergy/antagonism/additivity, two antibodies were used in combination. In all cases, one mAb was held at a constant concentration that on its own would be predicted to yield approximately 30% inhibition. A second mAb was then titrated alone to generate an inhibition curve. These data for the two mAbs (one titrated and one fixed concentration) are then used to

calculate the predicted GIA of the combination by Bliss additivity [38]. This prediction was then compared to the real GIA result of the mAb mixture tested in parallel using the combination concentration of the two mAbs (*i.e.* the fixed + titrated amounts).

Live cell imaging in the presence of antibodies which bind PfRH5 and PfCyRPA

Methods used are as described in [20], with the following exceptions: microscopy dishes used were 200 µL capacity, and the oxygen concentration used was 5% O_2. Concentrations of antibody used were as follows: EBL 040 400 µg/mL, R5.004 22 µg/mL and 200 µg/mL, R5.008 40 µg/mL, Cy.009 60 µg/mL and 200 µg/mL, Cy.003 250 µg/mL, Cy.007 Fab fragment 133 µg/mL and 400 µg/mL, Cy.007 IgG 400 µg/mL.

R5.004 and R5.008 are anti-PfRH5 human IgG1 mAbs and have been reported previously [4]. Cy.009, Cy.007 and Cy.003 were provided by Icosagen AS through the Centre for AIDS Reagents repository at the National Institute for Biological Standards and Control, UK. These mAbs were produced through the European Commission FP7 EURIPRED project [39]. Cy.009, Cy.007 and Cy.003 were produced by Icosagen using HybriFree Technology. For clarity, these mAbs were renamed from their original EURIPRED consortium catalogue names, which should be cited for reagent requests (Cy.009 = 7B9#13; Cy.003 = 3B3#17; Cy.007 = 3A7#22).

Statistical analysis

Data were analyzed using GraphPad Prism (GraphPad Software, version 9). For all unpaired t tests, two-tailed p values were considered significant if ≤ 0.05. Box and whisker plots indicate interquartile range with medians, and whiskers indicate minimum to maximum.

Acknowledgements

G.E.W. was recipient of NHMRC Early Career Research Fellowship. We thank the Australian Red Cross Blood Bank for providing blood and the Victorian Operational Infrastructure Support Program received by the Burnet Institute. We are grateful for support from NHMRC grant 1092789. R.J.R. was funded by a Rhodes scholarship; the Wellcome Trust Infection, Immunology and Translational Medicine D. Phil programme; and a Canadian Institutes of Health Research Doctoral Foreign Study Award (FRN:157835). B.G.W. held a UK MRC PhD Studentships (MR/N013468/1). S.J.D. held a Wellcome Trust Senior Fellowship (106917/Z/15/Z). Cy.003, Cy.007, and Cy.009 were provided by Icosagen AS through the Centre for AIDS Reagents repository at the National Institute for Biological Standards and Control, UK. These mAbs were produced through the European Commission FP7 EURIPRED project (INFRA-2012-312661), funded by the European Union's Seventh Framework Programme [FP7/2007—2013] under Grant Agreement No: 312661—European Research Infrastructures for Poverty Related Diseases (EURIPRED).

Competing interests

S.J.D. is a named inventor on patent applications relating to PfRH5 and/or other malaria vaccines and mAbs.

Author contributions

G.E.W., roles: Conceptualization, Data Curation, Formal Analysis, Investigation, Methodology, Validation, Visualization, Writing – Original Draft Preparation, Writing – Review & Editing; R.J.R., roles: Investigation, Writing – Review & Editing; D.Q., roles: Investigation; A.M.L., roles: Investigation; M.G.D., role: Investigation, Writing – Review & Editing. C.B., role: Investigation, Writing – Review & Editing; B.G.W., role: Investigation, Methodology; B.S.C., role: Funding acquisition. S.J.D., Project Administration, Resources, Supervision, Writing – Review & Editing. P.R.G., roles: Conceptualization, Data curation, Funding acquisition, Investigation, Methodology, Project Administration, Resources, Supervision, Writing – Review & Editing

References

1. World Health Organisation. World Malaria Report. 2022.

2. Cohen S, Butcher GA, Crandall RB. Action of malarial antibody *in vitro*. Nature. 1969;223. doi: 10.1038/223368a0.

3. Tran TM, Ongoiba A, Coursen J, Crosnier C, Diouf A, Huang CY, et al. Naturally acquired antibodies specific for *Plasmodium falciparum* reticulocyte-binding protein homologue 5 inhibit parasite growth and predict protection from malaria. J Infect Dis. 2014;209(5):789-98. Epub 2013/10/18. doi: 10.1093/infdis/jit553. PubMed PMID: 24133188; PubMed Central PMCID: PMCPMC3923542.

4. Alanine DGW, Quinkert D, Kumarasingha R, Mehmood S, Donnellan FR, Minkah NK, et al. Human Antibodies that Slow Erythrocyte Invasion Potentiate Malaria-Neutralizing Antibodies. Cell. 2019;178(1):216-28 e21. Epub 2019/06/18. doi: 10.1016/j.cell.2019.05.025. PubMed PMID: 31204103; PubMed Central PMCID: PMCPMC6602525.

5. Minassian AM, Silk SE, Barrett JR, Nielsen CM, Miura K, Diouf A, et al. Reduced blood-stage malaria growth and immune correlates in humans following RH5 vaccination. Med (N Y). 2021;2(6):701-19 e19. Epub 2021/07/06. doi: 10.1016/j.medj.2021.03.014. PubMed PMID: 34223402; PubMed Central PMCID: PMCPMC8240500.

6. Scally SW, Triglia T, Evelyn C, Seager BA, Pasternak M, Lim PS, et al. PCRCR complex is essential for invasion of human erythrocytes by *Plasmodium falciparum*. Nat Microbiol. 2022;7(12):2039-53. Epub 2022/11/19. doi: 10.1038/s41564-022-01261-2. PubMed PMID: 36396942; PubMed Central PMCID: PMCPMC9712106.

579 7. Ragotte RJ, Higgins MK, Draper SJ. The RH5-CyRPA-Ripr Complex as a Malaria Vaccine
580 Target. Trends Parasitol. 2020;36(6):545-59. Epub 2020/05/04. doi: 10.1016/j.pt.2020.04.003.
581 PubMed PMID: 32359873; PubMed Central PMCID: PMCPMC7246332.
582 8. Wong W, Huang R, Menant S, Hong C, Sandow JJ, Birkinshaw RW, et al. Structure of
583 *Plasmodium falciparum* Rh5-CyRPA-Ripr invasion complex. Nature. 2019;565(7737):118-21.
584 Epub 2018/12/14. doi: 10.1038/s41586-018-0779-6. PubMed PMID: 30542156.
585 9. Volz JC, Yap A, Sisquella X, Thompson JK, Lim NT, Whitehead LW, et al. Essential Role of
586 the PfRh5/PfRipr/CyRPA Complex during *Plasmodium falciparum* Invasion of Erythrocytes. Cell
587 Host Microbe. 2016;20(1):60-71. Epub 2016/07/05. doi: 10.1016/j.chom.2016.06.004. PubMed
588 PMID: 27374406.
589 10. Chen L, Lopaticki S, Riglar DT, Dekiwadia C, Uboldi AD, Tham WH, et al. An EGF-like protein
590 forms a complex with PfRh5 and is required for invasion of human erythrocytes by *Plasmodium*
591 *falciparum*. PLoS Pathog. 2011;7(9):e1002199. Epub 2011/09/13. doi:
592 10.1371/journal.ppat.1002199. PubMed PMID: 21909261; PubMed Central PMCID:
593 PMCPMC3164636.
594 11. Crosnier C, Bustamante LY, Bartholdson SJ, Bei AK, Theron M, Uchikawa M, et al. Basigin
595 is a receptor essential for erythrocyte invasion by *Plasmodium falciparum*. Nature. 2011;480.
596 12. Douglas AD, Williams AR, Illingworth JJ, Kamuyu G, Biswas S, Goodman AL, et al. The
597 blood-stage malaria antigen PfRH5 is susceptible to vaccine-inducible cross-strain neutralizing
598 antibody. Nat Commun. 2011;2:601. Epub 2011/12/22. doi: 10.1038/ncomms1615. PubMed
599 PMID: 22186897; PubMed Central PMCID: PMCPMC3504505.

600 13. Hayton K, Gaur D, Liu A, Takahashi J, Henschen B, Singh S, et al. Erythrocyte binding
601 protein PfRH5 polymorphisms determine species-specific pathways of *Plasmodium falciparum*
602 invasion. Cell Host Microbe. 2008;4(1):40-51. Epub 2008/07/16. doi:
603 10.1016/j.chom.2008.06.001. PubMed PMID: 18621009; PubMed Central PMCID:
604 PMCPMC2677973.
605 14. Baum J, Chen L, Healer J, Lopaticki S, Boyle M, Triglia T, et al. Reticulocyte-binding protein
606 homologue 5 - an essential adhesin involved in invasion of human erythrocytes by *Plasmodium*
607 *falciparum*. Int J Parasitol. 2009;39(3):371-80. Epub 2008/11/13. doi:
608 10.1016/j.ijpara.2008.10.006. PubMed PMID: 19000690.
609 15. Dreyer AM, Matile H, Papastogiannidis P, Kamber J, Favuzza P, Voss TS, et al. Passive
610 immunoprotection of *Plasmodium falciparum*-infected mice designates the CyRPA as candidate
611 malaria vaccine antigen. J Immunol. 2012;188(12):6225-37. Epub 2012/05/18. doi:
612 10.4049/jimmunol.1103177. PubMed PMID: 22593616.
613 16. Bjerkan L, Visweswaran GRR, Gudjonsson A, Labbe GM, Quinkert D, Pattinson DJ, et al.
614 APC-Targeted DNA Vaccination Against Reticulocyte-Binding Protein Homolog 5 Induces
615 *Plasmodium falciparum*-Specific Neutralizing Antibodies and T Cell Responses. Front Immunol.
616 2021;12:720550. Epub 2021/11/05. doi: 10.3389/fimmu.2021.720550. PubMed PMID:
617 34733274; PubMed Central PMCID: PMCPMC8558525.
618 17. Minassian AM, Themistocleous Y, Silk SE, Barrett JR, Kemp A, Quinkert D, et al. Controlled
619 human malaria infection with a clone of *Plasmodium vivax* with high-quality genome assembly.
620 JCI Insight. 2021;6(23). Epub 2021/10/06. doi: 10.1172/jci.insight.152465. PubMed PMID:
621 34609964; PubMed Central PMCID: PMCPMC8675201.

622 18. Murin CD, Gilchuk P, Crowe JE, Jr., Ward AB. Structural Biology Illuminates Molecular
623 Determinants of Broad Ebolavirus Neutralization by Human Antibodies for Pan-Ebolavirus
624 Therapeutic Development. Front Immunol. 2021;12:808047. Epub 2022/01/28. doi:
625 10.3389/fimmu.2021.808047. PubMed PMID: 35082794; PubMed Central PMCID:
626 PMCPMC8784787.
627 19. Ragotte RJ, Pulido D, Lias AM, Quinkert D, Alanine DGW, Jamwal A, et al. Heterotypic
628 interactions drive antibody synergy against a malaria vaccine candidate. Nat Commun.
629 2022;13(1):933. Epub 2022/02/19. doi: 10.1038/s41467-022-28601-4. PubMed PMID: 35177602;
630 PubMed Central PMCID: PMCPMC8854392 relating to PfRH5 and/or other malaria vaccines,
631 mAbs, and immunization regimes.
632 20. Weiss GE, Gilson PR, Taechalertpaisarn T, Tham WH, de Jong NW, Harvey KL, et al.
633 Revealing the sequence and resulting cellular morphology of receptor-ligand interactions during
634 *Plasmodium falciparum* invasion of erythrocytes. PLoS Pathog. 2015;11(2):e1004670. doi:
635 10.1371/journal.ppat.1004670. PubMed PMID: 25723550; PubMed Central PMCID:
636 PMCPMC4344246.
637 21. Rijal P, Elias SC, Machado SR, Xiao J, Schimanski L, O'Dowd V, et al. Therapeutic
638 Monoclonal Antibodies for Ebola Virus Infection Derived from Vaccinated Humans. Cell Rep.
639 2019;27(1):172-86 e7. Epub 2019/04/04. doi: 10.1016/j.celrep.2019.03.020. PubMed PMID:
640 30943399.
641 22. Dvorak JA, Miller LH, Whitehouse WC, Shiroishi T. Invasion of erythrocytes by malaria
642 merozoites. Science. 1975;187. doi: 10.1126/science.803712.

643 23. Gilson PR, Crabb BS. Morphology and kinetics of the three distinct phases of red blood
644 cell invasion by *Plasmodium falciparum* merozoites. Int J Parasitol. 2009;39(1):91-6. doi:
645 10.1016/j.ijpara.2008.09.007. PubMed PMID: 18952091.
646 24. Payne RO, Silk SE, Elias SC, Miura K, Diouf A, Galaway F, et al. Human vaccination against
647 RH5 induces neutralizing antimalarial antibodies that inhibit RH5 invasion complex interactions.
648 JCI Insight. 2017;2(21). Epub 2017/11/03. doi: 10.1172/jci.insight.96381. PubMed PMID:
649 29093263.
650 25. Jamwal A, Constantin C, Henrich S, W B, Fakler B, Draper S, et al. Erythrocyte invasion-
651 neutralising antibodies prevent *Plasmodium falciparum* RH5 from binding to basigin-containing
652 membrane protein complexes. bioRxiv. 2022. doi: https://doi.org/10.1101/2022.09.23.509221.
653 26. Triglia T, Scally SW, Seager BA, Pasternak M, Dagley LF, Cowman AF. Plasmepsin X
654 activates function of the PCRCR complex in *P. falciparum* by processing PfRh5 for binding to
655 basigin and invasion of human erythrocytes. Research Square. 2023. doi: DOI:
656 https://doi.org/10.21203/rs.3.rs-2410384/v1.
657 27. Geoghegan ND, Evelyn C, Whitehead LW, Pasternak M, McDonald P, Triglia T, et al. 4D
658 analysis of malaria parasite invasion offers insights into erythrocyte membrane remodeling and
659 parasitophorous vacuole formation. Nat Commun. 2021;12(1):3620. Epub 2021/06/17. doi:
660 10.1038/s41467-021-23626-7. PubMed PMID: 34131147; PubMed Central PMCID:
661 PMCPMC8206130.
662 28. Bannister LH, Butcher GA, Dennis ED, Mitchell GH. Structure and invasive behaviour of
663 *Plasmodium knowlesi* merozoites in vitro. Parasitology. 1975;71(3):483-91. Epub 1975/12/01.
664 doi: 10.1017/s0031182000047247. PubMed PMID: 1202413.

665 29. Pavlou G, Biesaga M, Touquet B, Lagal V, Balland M, Dufour A, et al. *Toxoplasma* Parasite
666 Twisting Motion Mechanically Induces Host Cell Membrane Fission to Complete Invasion within
667 a Protective Vacuole. Cell Host Microbe. 2018;24(1):81-96 e5. Epub 2018/07/17. doi:
668 10.1016/j.chom.2018.06.003. PubMed PMID: 30008293.
669 30. Healer J, Thompson JK, Mackwell KL, Browne CD, Seager BA, Ngo A, et al. RH5.1-CyRPA-
670 Ripr antigen combination vaccine shows little improvement over RH5.1 in a preclinical setting.
671 Front Cell Infect Microbiol. 2022;12:1049065. Epub 2023/01/07. doi:
672 10.3389/fcimb.2022.1049065. PubMed PMID: 36605129; PubMed Central PMCID:
673 PMCPMC9807911.
674 31. Boyle MJ, Wilson DW, Richards JS, Riglar DT, Tetteh KKA, Conway DJ, et al. Isolation of
675 viable *Plasmodium falciparum* merozoites to define erythrocyte invasion events and advance
676 vaccine and drug development. Proceedings of the National Academy of Sciences.
677 2010;107(32):14378-83. doi: 10.1073/pnas.1009198107.
678 32. Besteiro S, Michelin A, Poncet J, Dubremetz JF, Lebrun M. Export of a *Toxoplasma gondii*
679 rhoptry neck protein complex at the host cell membrane to form the moving junction during
680 invasion. PLoS Pathog. 2009;5(2):e1000309. Epub 2009/02/28. doi:
681 10.1371/journal.ppat.1000309. PubMed PMID: 19247437; PubMed Central PMCID:
682 PMCPMC2642630.
683 33. Riglar DT, Richard D, Wilson DW, Boyle MJ, Dekiwadia C, Turnbull L, et al. Super-
684 Resolution Dissection of Coordinated Events during Malaria Parasite Invasion of the Human
685 Erythrocyte. Cell Host & Microbe. 2011;9(1):9-20. doi: 10.1016/j.chom.2010.12.003.

686 34. Tonkin ML, Roques M, Lamarque MH, Pugniere M, Douguet D, Crawford J, et al. Host cell
687 invasion by apicomplexan parasites: insights from the co-structure of AMA1 with a RON2 peptide.
688 Science. 2011;333(6041):463-7. doi: 10.1126/science.1204988. PubMed PMID: 21778402.
689 35. Malkin E, Long CA, Stowers AW, Zou L, Singh S, MacDonald NJ, et al. Phase 1 study of two
690 merozoite surface protein 1 (MSP1(42)) vaccines for *Plasmodium falciparum* malaria. PLoS Clin
691 Trials. 2007;2(4):e12. doi: 10.1371/journal.pctr.0020012. PubMed PMID: 17415408; PubMed
692 Central PMCID: PMCPMC1847697.
693 36. Malkin EM, Diemert DJ, McArthur JH, Perreault JR, Miles AP, Giersing BK, et al. Phase 1
694 clinical trial of apical membrane antigen 1: an asexual blood-stage vaccine for *Plasmodium*
695 *falciparum* malaria. Infect Immun. 2005;73(6):3677-85. Epub 2005/05/24. doi:
696 10.1128/IAI.73.6.3677-3685.2005. PubMed PMID: 15908397; PubMed Central PMCID:
697 PMCPMC1111886.
698 37. Douglas AD, Williams AR, Knuepfer E, Illingworth JJ, Furze JM, Crosnier C, et al.
699 Neutralization of *Plasmodium falciparum* merozoites by antibodies against PfRH5. J Immunol.
700 2014;192(1):245-58. Epub 2013/12/03. doi: 10.4049/jimmunol.1302045. PubMed PMID:
701 24293631; PubMed Central PMCID: PMCPMC3872115.
702 38. Bliss C. The toxicity of poisons applied jointly. Ann Appl Biol 1939;26:585–615.
703 39. Nacer A, Kivi G, Pert R, Juronen E, Holenya P, Aliprandini E, et al. Expanding the Malaria
704 Antibody Toolkit: Development and Characterisation of *Plasmodium falciparum* RH5, CyRPA, and
705 CSP Recombinant Human Monoclonal Antibodies. Front Cell Infect Microbiol. 2022;12:901253.
706 Epub 2022/07/06. doi: 10.3389/fcimb.2022.901253. PubMed PMID: 35782147; PubMed Central
707 PMCID: PMCPMC9243361.

708 40. Wright KE, Hjerrild KA, Bartlett J, Douglas AD, Jin J, Brown RE, et al. Structure of malaria
709 invasion protein RH5 with erythrocyte basigin and blocking antibodies. Nature.
710 2014;515(7527):427-30. Epub 2014/08/19. doi: 10.1038/nature13715. PubMed PMID:
711 25132548; PubMed Central PMCID: PMCPMC4240730.

712

713

Figure Legends

Fig 1 The major stages of invasion of *Plasmodium falciparum* blood stage parasites and growth inhibitory activity (GIA) of anti-PfRH5 and -PfCyRPA IgGs and Fab fragments. (A) Several videos of *P. falciparum* in the presence of 400 µg/mL EBL 040 control IgG were analyzed to derive the average times for each of the major steps of pre-invasion, internalization, merozoite to ring transition and echinocytosis (EC) of the infected erythrocyte. After egress, merozoites took 42.0 s to contact the erythrocyte they invaded (all times are means). Following an initial contact of 0.9 s, the merozoites deformed their erythrocytes for 52.6 s followed by the quiescent complex stage of 1.8 s, when it is believed the PCRCR complex and tight junction form ("Rh5-basigin stage"). Merozoite internalization or invasion takes 10.3 s after which the merozoite starts to spin 16.4 s later. Spinning lasts 116.3 s and once finished, a pseudopod emerges from the merozoite 159.2 s later. 57.2 s after this, the merozoite membrane starts to become irregular and by 638 s a fully formed amoeboid ring is evident. 41 s after invasion is complete, the host erythrocyte develops membranous protrusions in a process called echinocytosis. These protrusions increase in their extent reaching a maximum after 42 s. This state continues for 395.9 s until the erythrocyte returns to its usual biconcave shape. Of note, the timing and duration of echinocytosis is highly variable. (B) *In vitro* single cycle growth inhibition activity (GIA) assay dilution series of R5.008 mAb alone (pink), or in combination with Cy.009 mAb held at 0.13 mg/mL (blue), against 3D7 parasites. Predicted Bliss additivity is indicated (grey). The solid green line indicates the GIA of mAb Cy.009 held alone at a fixed concentration of 0.13 mg/mL. Dotted line indicates 50% GIA. (C) Comparison of the GIA of the Cy.007 mAb (purple) with its Fab fragment (light pink) indicating the latter is much more potent. Assay performed as in B.

Fig 2. Parasite specific mAbs to PfRH5 and PfCyRPA inhibit *Plasmodium falciparum* invasion of human erythrocytes. (A-F) Several live cell videos of *P. falciparum* merozoites egressing and attempting to invade erythrocytes in the presence of each of the antibody (concentrations and combinations indicated) were analyzed. The number of successful events is presented for each parameter indicated by the y axis. Full antibody names and concentrations (µg/mL) are indicated below bottom graphs. The boxes indicate the median number of events (A,B,E) or the percentage of events (C,D,F) and the 25% to 75% percentile, and whiskers show the range. Statistical analyses were performed using unpaired t tests in GraphPad PRISM V 9.0. The asterisks indicate where parasite mAbs have altered the number/percentage of events significantly from the EBL 040 control with *p<0.05, **p<0.01 and ***p<0.001.

Fig 3. Antibodies to PfRH5 and PfCyRPA modify temporal aspects of the pre- and post-invasion phases of *Plasmodium falciparum* into human erythrocytes. (A-E) The invasion steps being monitored from live cell videos of antibody-treated parasites are indicated on the y-axes. The antibody types and concentrations are indicated on the x-axes. Anti-PfRH5 (orange, pink) and Cy.009 (green) antibodies tend to increase the length of the preinvasion phase from first erythrocyte contact to the start of merozoite penetration. The Cy.003 (dark blue) and Cy.007 IgG and Fabs (purples) tend to increase the length of the merozoite internalization period. (F) Cy.007 antibodies decrease the numbers of echinocytosis events per egress and (G-H) R5.008 (pink) and Cy.009 (green) decrease the time from the end of invasion/deformation to

758 echinocytosis. Full antibody names and concentrations (µg/mL) are indicated below bottom
759 graphs. Antibody 8 indicates Cy.007 Fab-(133). The boxes indicate the median number of events
760 and the 25% to 75% percentile, and whiskers show the range. Statistical analyses were
761 performed using unpaired t tests in GraphPad PRISM V 9.0. The asterisks indicate where
762 parasite mAbs have altered the number of events significantly from the EBL 040 control with
763 *p<0.05, **p<0.01 and ***p<0.001.

764

765 **Fig 4. The effects of anti-PfRH5 and PfCyRPA antibodies upon the differentiation of**
766 **intracellular and extracellular merozoites into ring-stage parasites.** (A-C) The ability of the
767 antibodies to stimulate or inhibit the differentiation of intracellular, extracellular and regressed
768 merozoites into (A) early, (B) preliminary and (C) complete ring-stage parasites was assessed
769 from observing live cell imaging videos of *Plasmodium falciparum* parasites. Full antibody
770 names and concentrations (µg/mL) are indicated below bottom graph. The boxes indicate the
771 median number of events and the 25% to 75% percentile, and whiskers show the range.
772 Statistical analyses were performed using unpaired t tests in GraphPad PRISM V 9.0. The
773 asterisks indicate where parasite mAbs have altered the number of events significantly from
774 the EBL 040 intracellular or extracellular control (arrows) with *p<0.05, **p<0.01 and
775 ***p<0.001. (D) Diagram summarizing the effects of the anti-PfRH5 and -PfCyRPA antibodies
776 upon ring differentiation for intracellular and extracellular merozoites.

777

Supplementary Figures

S1 Fig Epitopes recognized by anti-PfRH5 and -PfCyRPA Fabs and the growth inhibitory activity of PfCyRPA Fabs against the *Plasmodium falciparum* asexual blood stage. (A) Crystal structure of PfRH5 bound to basigin (protein data bank (PDB) ID: 4U0Q [40]). (B) Crystal structure of PfRH5 bound to R5.004 (PDB ID: 6RCU [4]). No structure of R5.008 is available, however both R5.004 and R5.008 compete with basigin for binding but do not compete with each other [4]. (C) Crystal structure of PfCyRPA bound to Cy.003, Cy.004, and Cy.007 (PDB ID: 7PI3 [19]). No structure is available for Cy.009 however Cy.004 and Cy.009 bind overlapping epitopes [19]. (D) Location of PfRH5 and PfCyRPA mAbs used in this study in the context of the PfRH5 (yellow), PfCyRPA (blue), PfRIPR (green) complex bound to basigin (composite image using PDB ID: 6MPV [8] & 4U0Q [40]). (E and F) Schizont stage *Plasmodium falciparum* 3D7 parasites were incubated with a micromolar dilution series of monoclonal antibodies (mAbs) and Fab fragments of Cy.003 and Cy.009 and grown for 40 h before parasite growth inhibitory activity (GIA) was quantified by measuring lactate dehydrogenase activity. (G) Comparison of GIA activities of anti-PfCyRPA Fabs.

S2 Fig Quantification of the effects of antibodies to PfRH5 and PfCyRPA upon the invasion of erythrocytes by *Plasmodium falciparum* 3D7 merozoites. Video microscopy of several merozoite egress events was observed in the presence of antibodies with concentrations in

798 µg/mL indicated in brackets. (A) The times from egress to first contact indicate were not
799 significantly different indicating the imaging conditions were consistent. (B) The degree of
800 deformation of merozoites on erythrocyte surfaces was quantified according to [20] in the
801 presence of antibodies. R5.004-(22) caused significantly less deformation than the control or
802 parasite antibodies using. (C-G) The timings of other invasion stage as indicated on the y-axes
803 were measured using the antibody combinations names and concentrations (µg/mL) indicated
804 below the x-axes. Antibody 8 is Cy.007 Fab-(133) and 8+ is Cy.007 Fab-(400). The boxes indicate
805 the median number of events and the 25% to 75% percentile, and whiskers show the range.
806 Statistical analyses were performed using unpaired t tests in GraphPad PRISM V 9.0. The
807 asterisks indicate where parasite mAbs have altered the number of events significantly from
808 the EBL 040 control with *p<0.05, **p<0.01 and ***p<0.001.

809

810 **S3 Fig 5 Anti-PfRH5 and -PfCyRPA antibodies influence the speed with which intracellular and**
811 **extracellular merozoites differentiate into rings.** (A) The speed with which merozoites started
812 spinning after egress, (B) their duration of spinning, (C) from the end of spinning to pseudopod
813 appearance, (D) pseudopod formation to disruption of merozoites surface until (E) complete
814 ring formation respectively, were measured from live cell videos of cultured *Plasmodium*
815 *falciparum*. Full antibody names and concentrations (µg/mL) are indicated below bottom graph.
816 The boxes indicate the median number of events and the 25% to 75% percentile, and whiskers
817 show the range. Statistical analyses were performed using unpaired t tests in GraphPad PRISM
818 V 9.0. The asterisks indicate where parasite mAbs have altered the number of events

819 significantly from the intracellular and extracellular EBL 040 controls with *p<0.05, **p<0.01
820 and ***p<0.001.

821

822

823 **Supplementary videos**

824 **S1 Video EBL 040-(400). Live cell video of *Plasmodium falciparum* merozoites egressing from**
825 **schizont in the presence of control EBL 040 IgG at 400 µg/mL.** First appearance of white arrow
826 indicates merozoite invading erythrocyte and second appearance indicates differentiation of
827 this merozoite into a ring stage form. Note, an invasion was chosen in which the invaded red
828 blood cell did undergo echinocytosis so the merozoite's development into a ring-stage parasite
829 can be observed. Video playback is 10x live imaging speed.

830

831 **S2 Video R5.004-(22). Live cell video of *Plasmodium falciparum* merozoites egressing from**
832 **schizont in the presence of R5.004 IgG at 22 µg/mL.** There are no erythrocyte invasions
833 observed and black arrows indicates selected extracellular merozoites that are about to
834 differentiate into amoeboid ring-like forms beginning about 3 minutes after egress. Video
835 playback is 10x live imaging speed.

836

837 **S3 Video R5.008-(40). Live cell video of *Plasmodium falciparum* merozoites egressing from**
838 **schizont in the presence of R5.008 IgG at 40 µg/mL.** Successful invasions are indicated with
839 white arrows and black arrows indicate selected extracellular merozoites that begin to
840 differentiate into amoeboid ring-like forms beginning about 5:40 minutes after egress. Video
841 playback is 10x live imaging speed.

842

843 **S4 Video Cy.009-(60). Live cell video of *Plasmodium falciparum* merozoites egressing from**
844 **schizont in the presence of Cy.009 IgG at 60 µg/mL.** No successful invasions were detected and
845 the extracellular merozoites were observed to spin and begin to differentiate into amoeboid
846 ring-like forms about 4 minutes after egress. Video playback is 10x live imaging speed.

847

848 **S5 Video Cy.009-(200). Live cell video of *Plasmodium falciparum* merozoites egressing from**
849 **schizont in the presence of Cy.009 IgG at 200 µg/mL.** A successful invasion is indicated with a
850 white arrow and note how long the invasion takes to commence after the merozoite makes first
851 with its target erythrocyte. Black arrows indicate some of the extracellular merozoites that
852 begin to differentiate into amoeboid ring-like forms about 5 minutes after egress. Video
853 playback is 10x live imaging speed.

854

855 **S6 Video R5.008-(40) Cy.009-(200). Live cell video of *Plasmodium falciparum* merozoites**
856 **egressing from schizont in the presence of R5.008 IgG at 40 µg/mL and Cy.009 IgG at 200**

µg/mL. White arrow indicates one successful invasion with an extended pre-invasion period. Black arrows indicate selected extracellular merozoites that begin to change into amoeboid ring-like forms at about 4 minutes post egress. Video playback is 10x live imaging speed.

S7 Video Cy.003-(250). Live cell video of *Plasmodium falciparum* merozoites egressing from schizont in the presence of Cy.003 IgG at 250 µg/mL. A successful merozoite invasion is indicated with a white arrow and at 17 s the time from the start to the end of invasion is longer than the control (10 s). Extracellular merozoites generally remained unchanged during the 10 minutes observation period. Video playback is 10x live imaging speed.

S8 Video Cy.007 Fab-(133). Live cell video of *Plasmodium falciparum* merozoites egressing from schizont in the presence of Cy.007 Fab at 133 µg/mL. No merozoite invasions were observed and most extracellular merozoites did not change during the 10 min imaging period. Video playback is 10x live imaging speed.

S9 Video Cy.007 Fab-(400). Live cell video of *Plasmodium falciparum* merozoites egressing from schizont in the presence of Cy.007 Fab at 400 µg/mL. No merozoite invasions were observed and most extracellular merozoites did not change during the 10 min imaging period. Video playback is 10x live imaging speed.

S10 Video Cy.007-(400). Live cell video of *Plasmodium falciparum* merozoites egressing from schizont in the presence of Cy.007 IgG at 400 µg/mL. No merozoite invasions were observed and most extracellular merozoites did not change during the 10 min imaging period. Video playback is 10x live imaging speed.

S11 Video Cy.003-(250) Live cell video of *Plasmodium falciparum* merozoite regressing from invaded erythrocyte in the presence of Cy.003 IgG at 250 µg/mL. Merozoite invading erythrocyte is indicated with a white arrow which changes to block to show the merozoite regressing from the erythrocyte. Video playback is 10x live imaging speed.

Figure 1

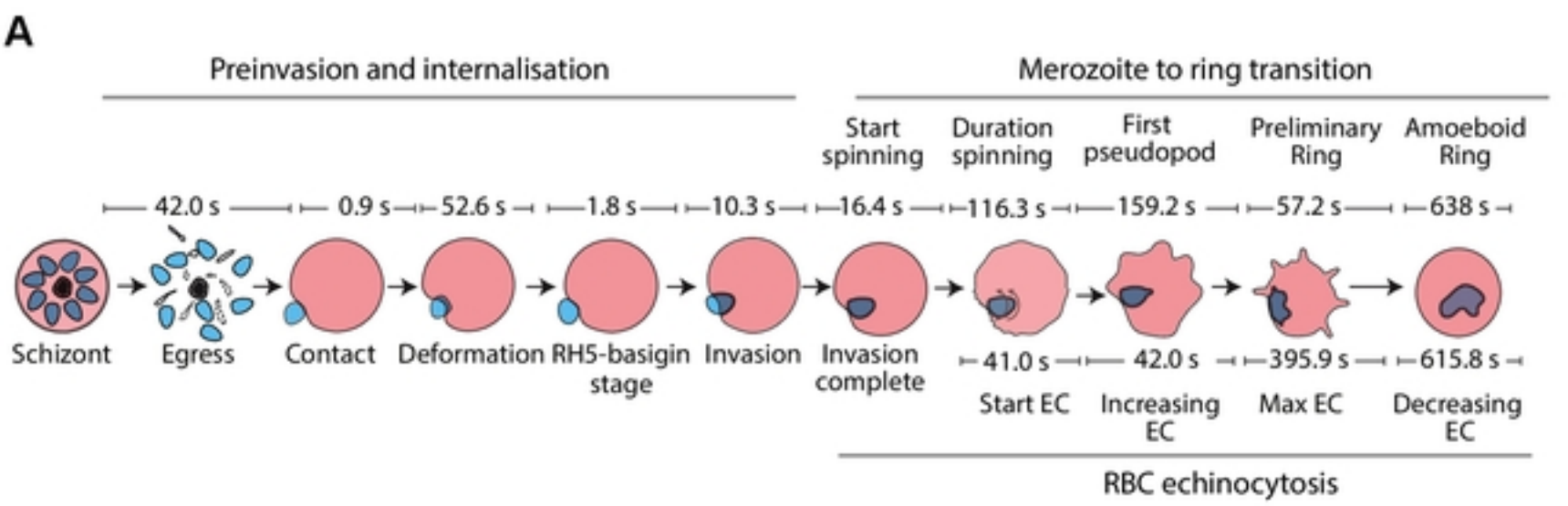

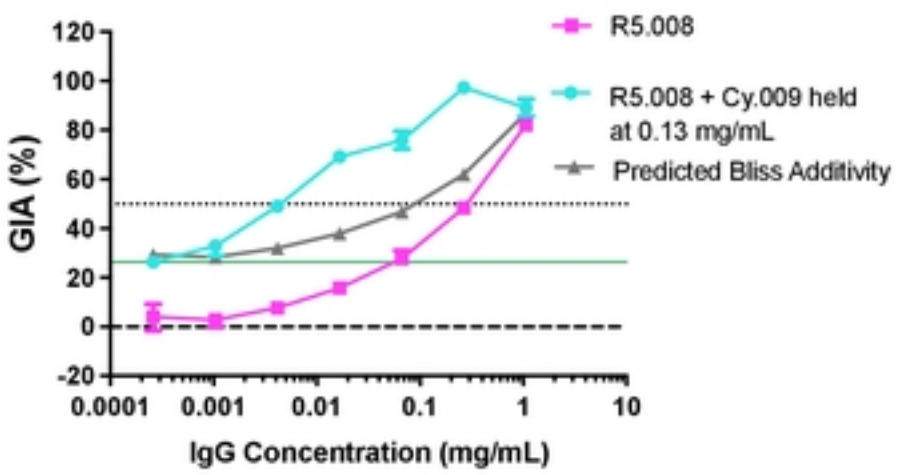

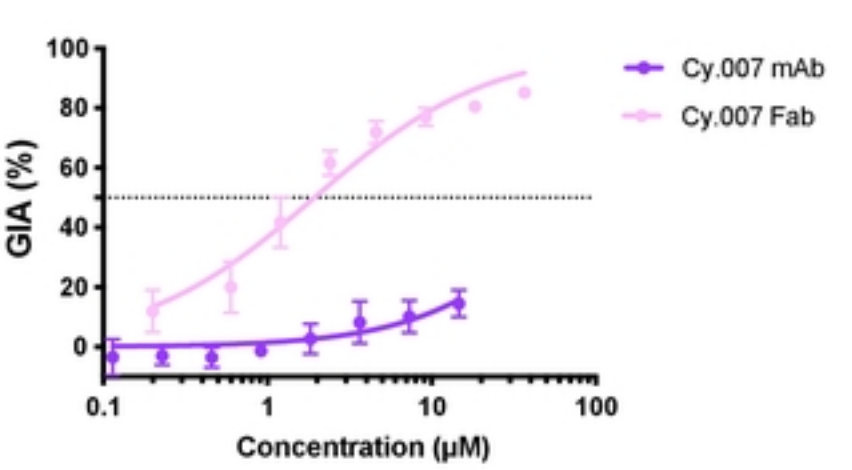

Figure 2

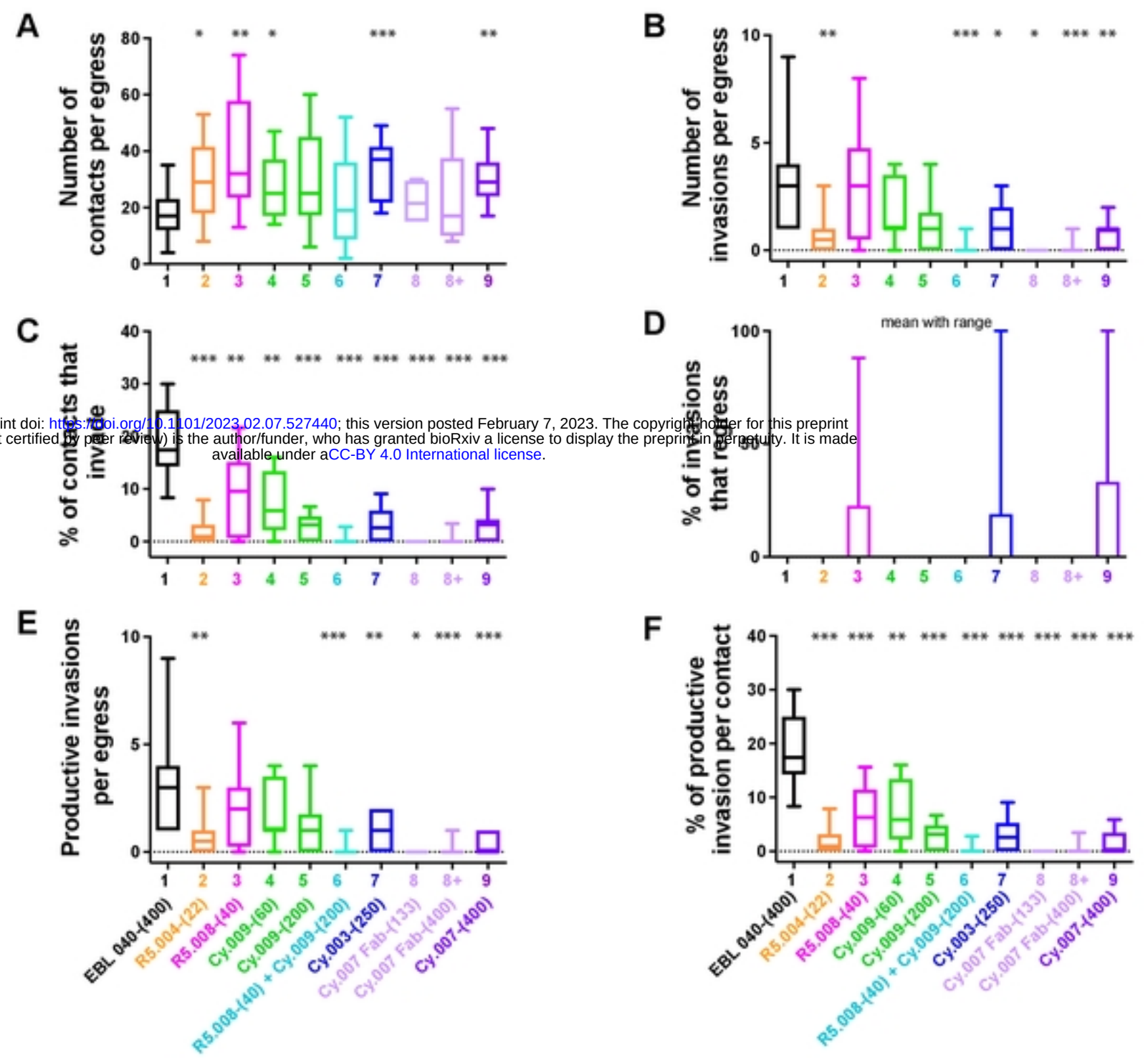

Figure 3

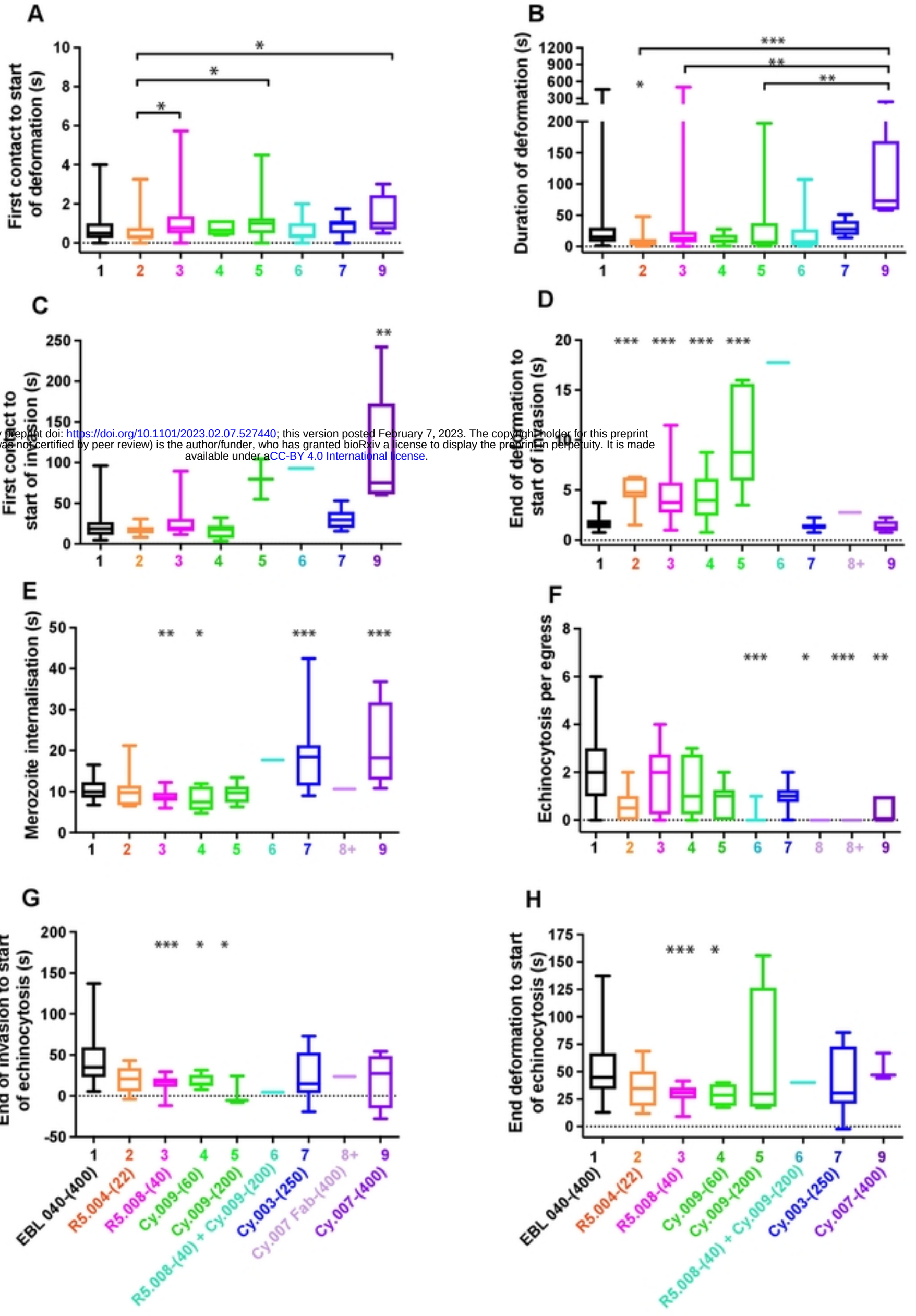

Fig 4

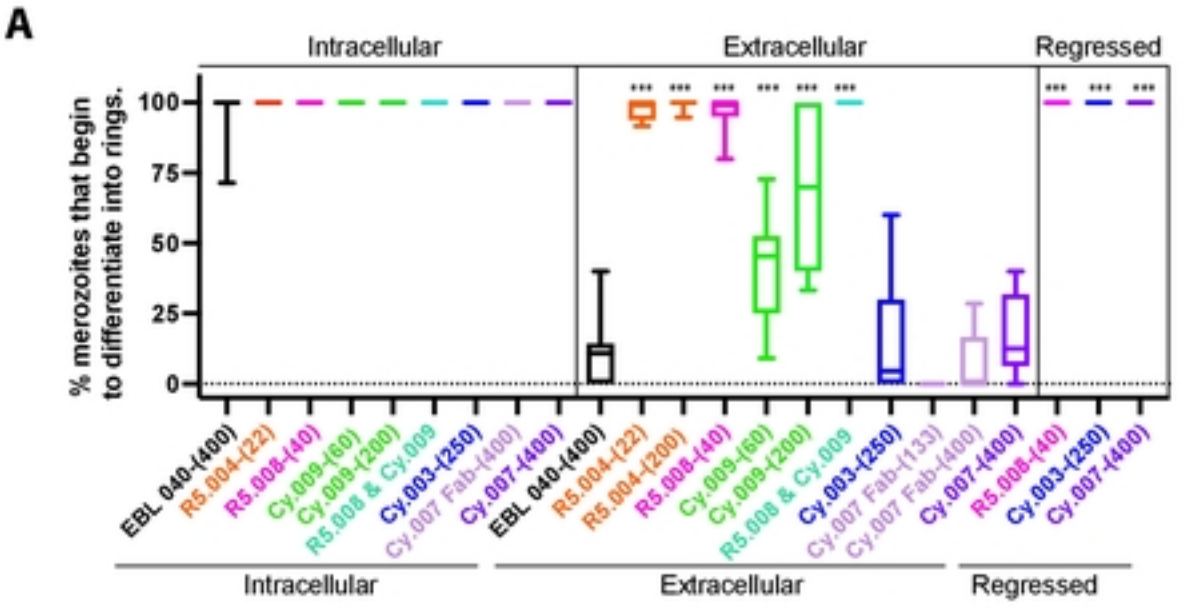

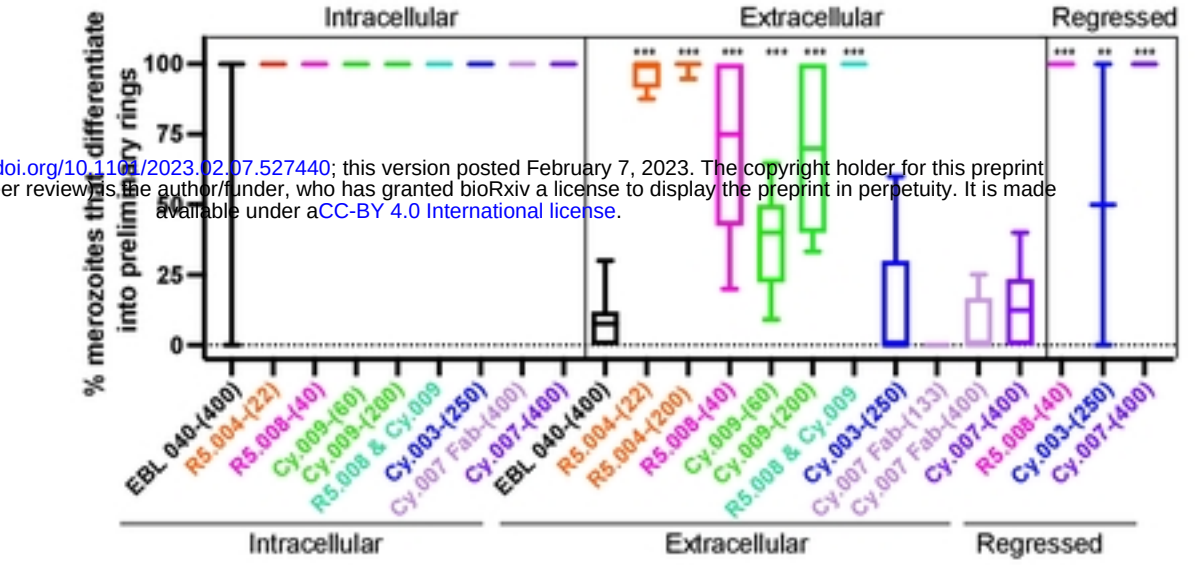

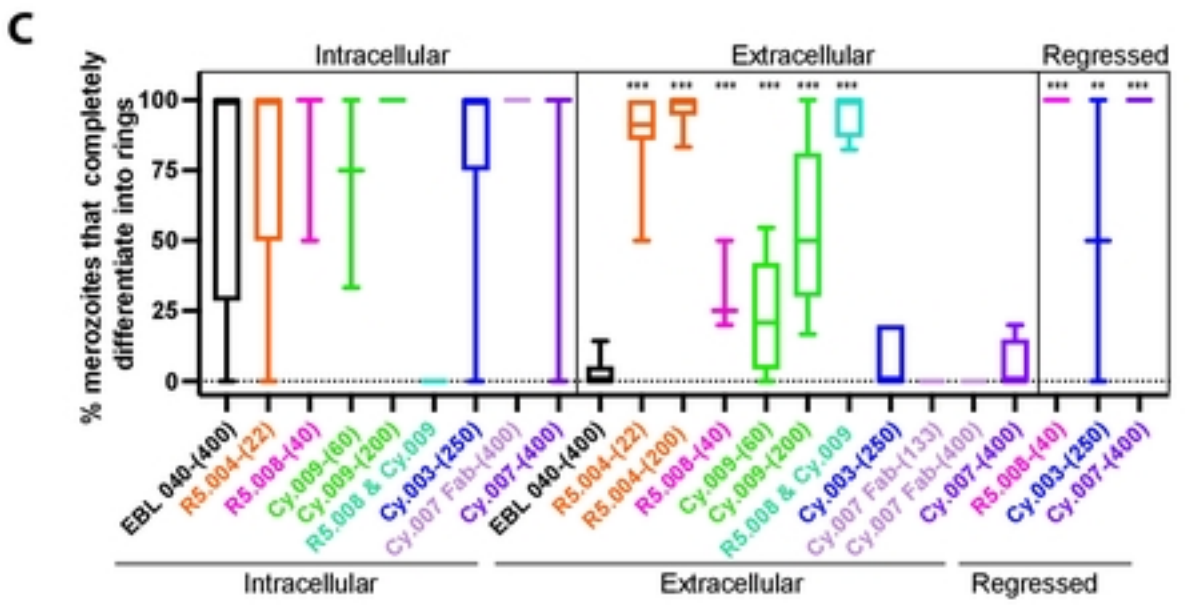

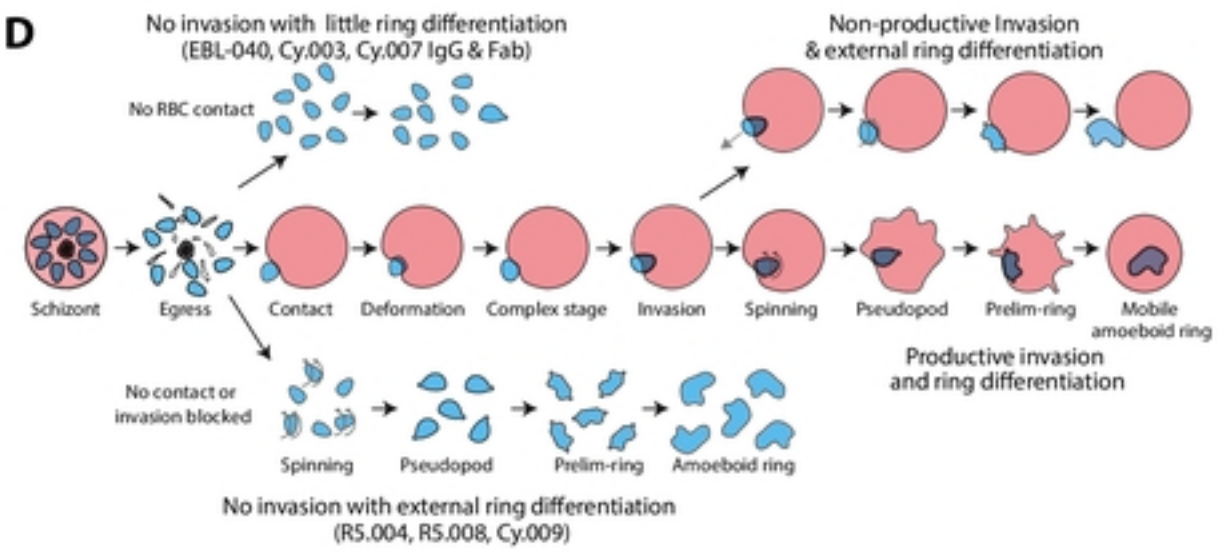

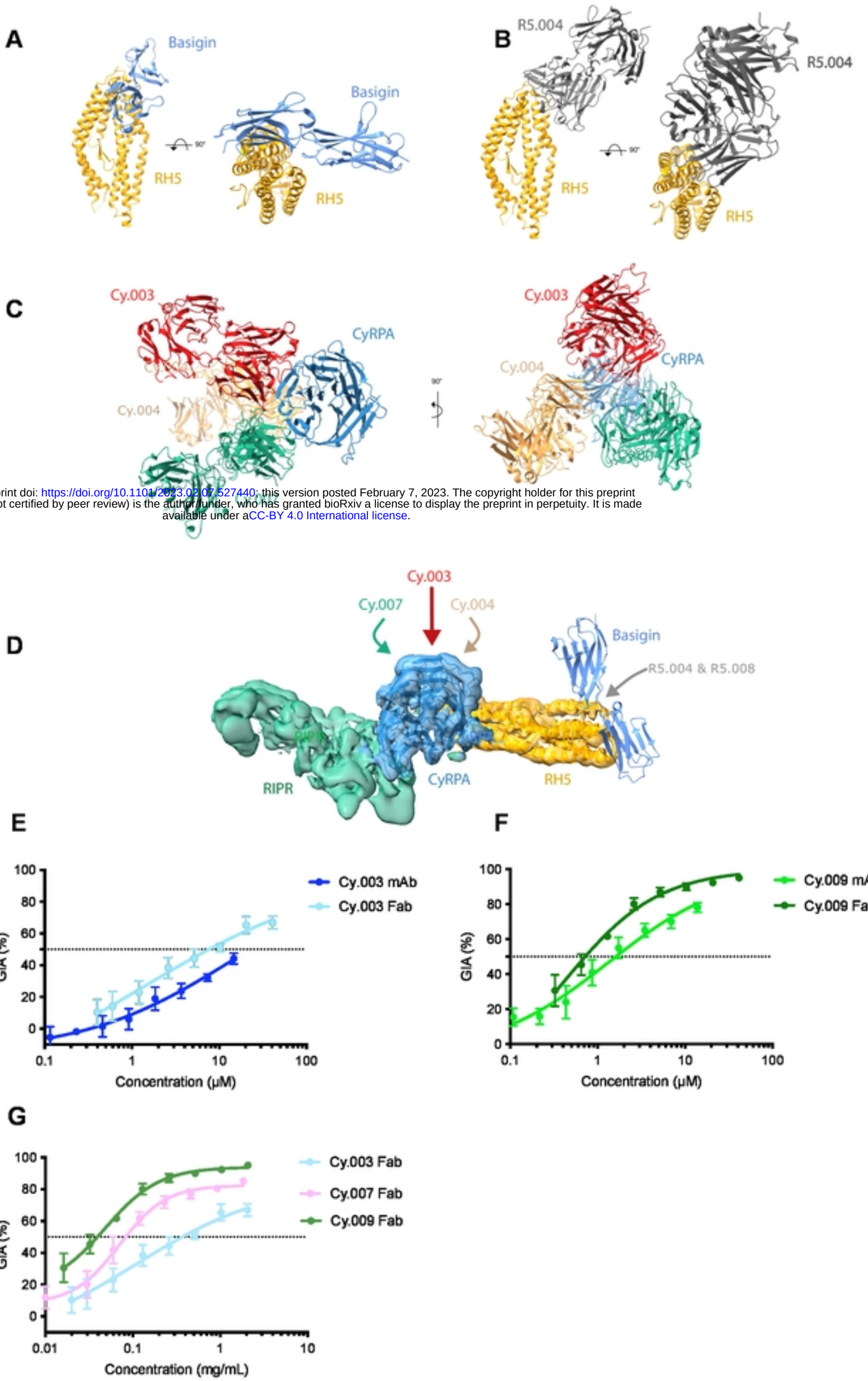

S1 Fig. Epitopes recognized by anti-PfRH5 and -PfCyRPA Fabs and the growth inhibitory activity of PfCyRPA Fabs against the *Plasmodium falciparum* asexual blood stage.

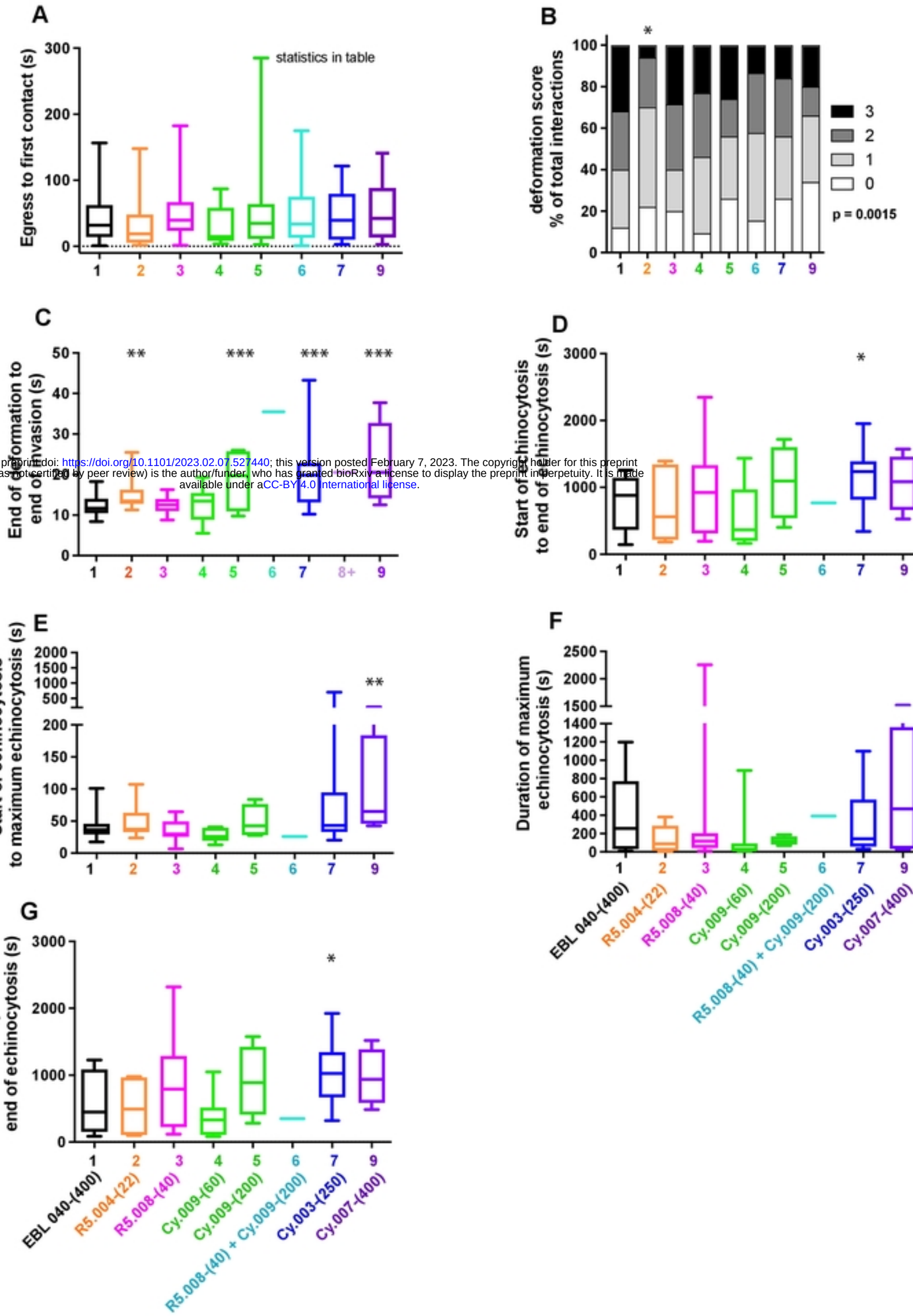

S2 Fig Quantification of the effects of antibodies to PfRH5 and PfCyRPA upon the invasion of erythrocytes by *Plasmodium falciparum* 3D7 merozoites.

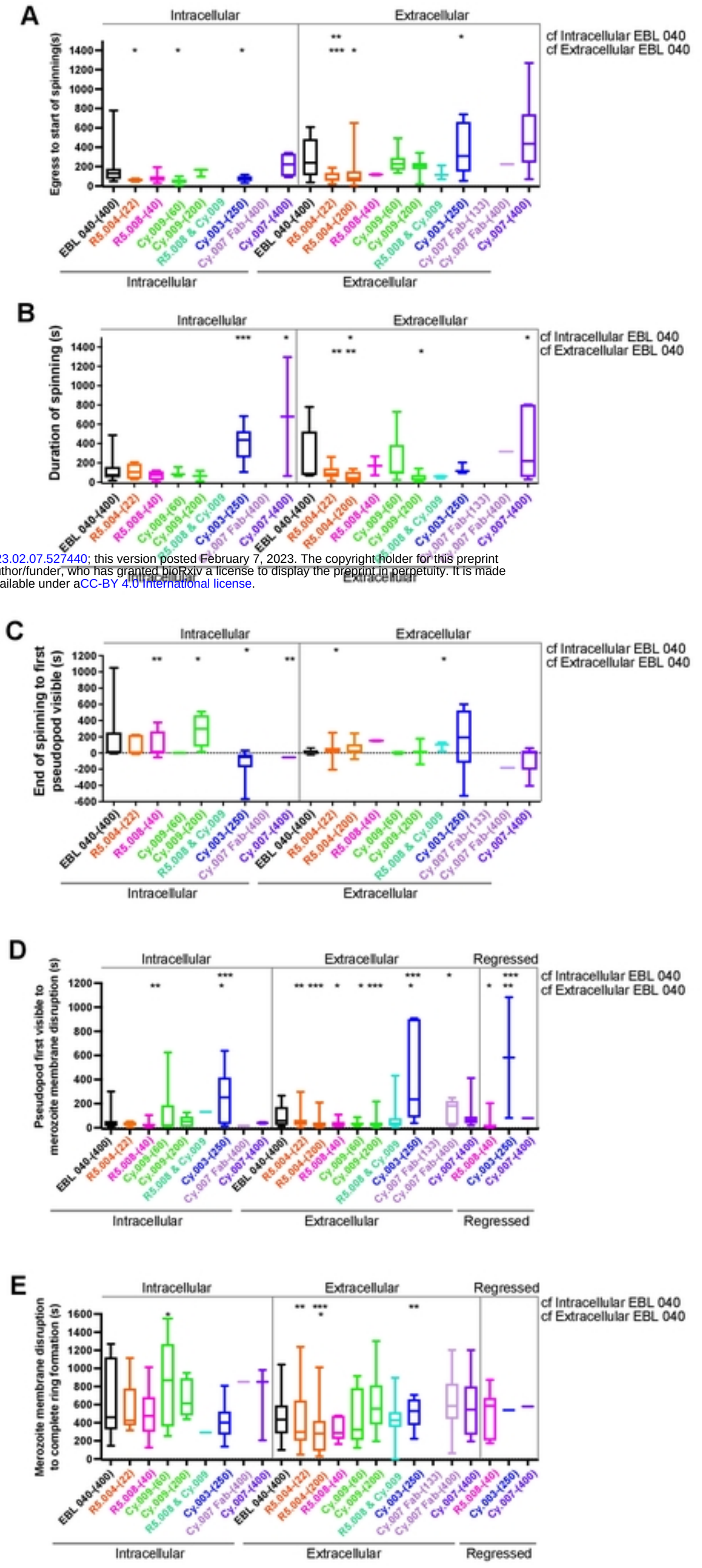

S3 Fig 5 Anti-PfRH5 and -PfCyRPA antibodies influence the speed with which intracellular and extracellular merozoites differentiate into rings.